Domino Reactions

International Edition: DOI: 10.1002/anie.201813829
German Edition: DOI: 10.1002/ange.201813829

Tracking the Process of a Solvothermal Domino Reaction Leading to a Stable Triheteroarylmethyl Radical: A Combined Crystallographic and Mass-Spectrometric Study

*Bin Liu[+], Fei Yu[+], Min Tu, Zhong-Hong Zhu, Yuexing Zhang, Zhong-Wen Ouyang, Zhenxing Wang, and Ming-Hua Zeng**

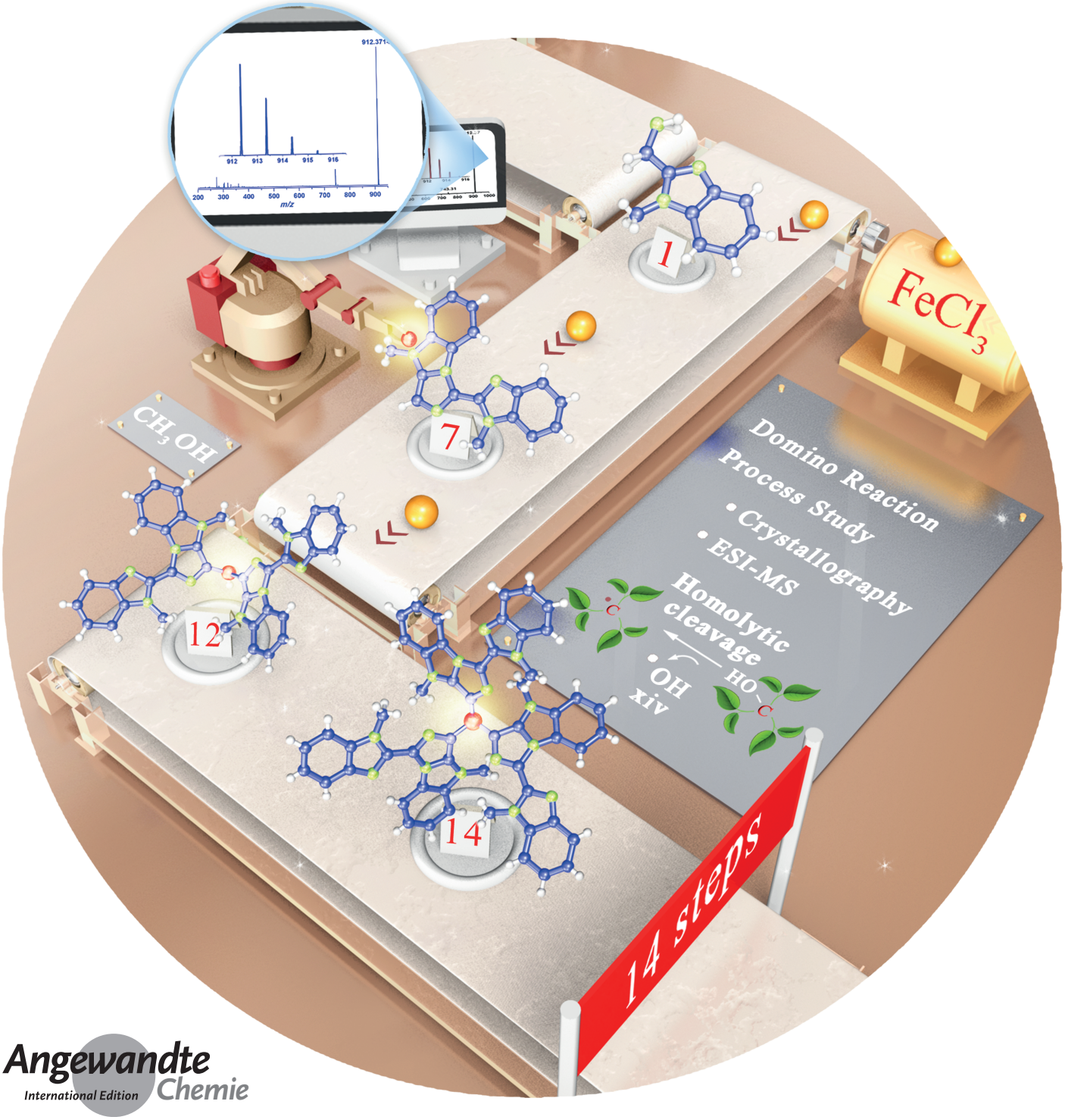

Abstract: *A new free carbon radical was obtained in a microwave-assisted solvothermal reaction of the primary amine (1-methyl-1H-benzo[d]imidazol-2-yl)methanamine with $FeCl_3{\cdot}6H_2O$ in methanol at 140°C. Through a combination of crystallography and electrospray ionization mass spectrometry, the reaction process was studied. The longest domino reaction includes 14 steps and forms up to 12 new covalent bonds (9 C–N and 3 C–C bonds) and 3 five-membered heterocycles. For the first time, the homolytic cleavage of a C–O bond was used to synthesize a triarylmethyl radical.*

One of the primary goals in chemistry is to understand bonding and the way reactions progress.[1–3] Domino reactions consist of multiple transformation steps in which the subsequent reaction takes place at the functional group formed in the previous step.[4–6] Molecules with complex architectures can be obtained from simple substrates by domino reactions without isolation of the intermediates, which improves atom economy.[5] Furthermore, domino reactions can also give molecules that cannot be produced by traditional methods, and as a result, they have been applied in many fields such as total synthesis and biology. Consequently, developing new domino reactions is very desirable (see the Supporting Information, Scheme S1), and tracking and understanding domino reactions is even more significant and challenging.

Under solvothermal conditions, some organic ligands can be transformed in situ into new ligands, in processes catalyzed by transition metals.[6,7] These "black box" conditions render it even more difficult to track and understand the overall process. Fortunately, combinations of techniques, such as crystallography and electrospray ionization mass spectrometry (ESI-MS), have been cooperatively applied in the study of complicated reaction processes.[2,6,8,9] For example, we have analyzed the process of a multistep assembly along with an in situ ligand reaction that gives a highly stable luminescent Zn_5 cluster,[8] as well as the generation of the biggest chiral cobalt coordination cluster Co_{16},[9a] and the heptanuclear disks Co_xNi_{7-x} ($x = 0$–7).[9b,c] Recently, we have discovered a $FeSO_4{\cdot}7H_2O$ catalyzed domino N-alkylation reaction of NEt_3/NH_3 under solvothermal conditions resulting in a trimeric cluster $[Fe_3(\mathbf{L_3}\text{-}N)_2]$.[6] The various Fe^{II} intermediates were identified by ESI-MS for the first time, and a mechanism was proposed with the help of crystallography. Furthermore, on this basis, we were able to selectively synthesize the organic intermediates by controlling the reaction time.

Herein, we describe the generation of a rare room-temperature-stable organic free radical, compound **1**, in a domino reaction under solvothermal conditions. In addition, key intermediates identified as "tetramer" **2**, "dimer" **3**, and $[Fe^{III}(\mathbf{L1})_2Cl(OCH_3)]Cl$ **4** were characterized by crystallography and ESI-MS (Scheme 1). Based on the structures of these intermediates, time-dependent ESI-MS of the reaction solution, control experiments, and isotope labeling experiments, a possible domino process was proposed. This is the longest one-pot domino reaction reported thus far, involving up to 14 steps and constructing 12 new covalent bonds (9 C–N and 3 C–C bonds) and three five-membered heterocycles.

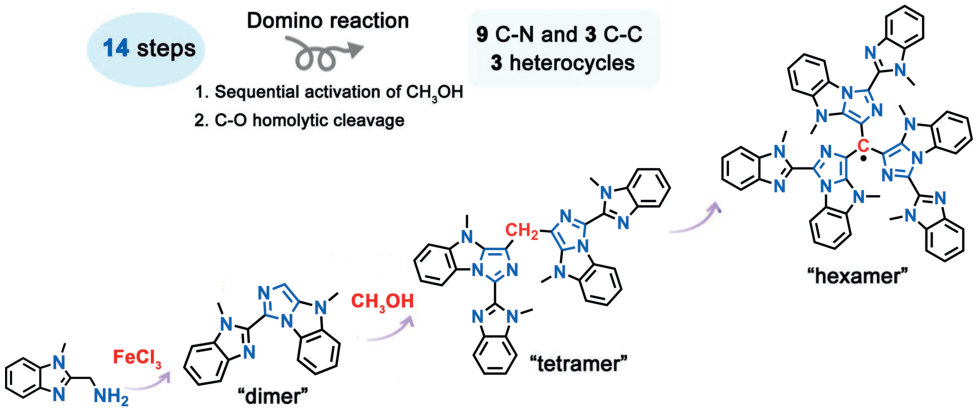

Scheme 1. The chemical structures of **L1**, "dimer" **3**, "tetramer" **2**, and "hexamer" **1** formed during the domino reaction leading to compound **1**.

Ligand **L1** (1-methyl-1*H*-benzo[*d*]imidazol-2-yl)methanamine (1 mmol) was dissolved in methanol (20 mL) at room temperature followed by the addition of $FeCl_3{\cdot}6H_2O$ (0.2 mmol). The reaction mixture was stirred for 10 min and then transferred to a Teflon-lined steel bomb and subjected to microwave heating at 140 °C for 30 min. The reaction mixture was evaporated to dryness, the residue was dissolved in CH_2Cl_2, and the resulting suspension was filtered to give a blue solution from which purple solid **1** was obtained by column chromatography (EtOAc/MeOH = 3:1) in 30 % yield (based on **L1**).

Compound **1** ($C(C_{18}H_{14}N_5)HCl{\cdot}3\,CH_3OH$) crystallizes in the orthorhombic space group $Pna2_1$ with a chloride counter-

[*] Dr. B. Liu,[+] M. Tu, Dr. Y. Zhang, Dr. M.-H. Zeng
Hubei Collaborative Innovation Center for Advanced Organic Chemical Materials, Ministry of Education Key Laboratory for the Synthesis and Application of Organic Functional Molecules
College of Chemistry and Chemical Engineering, Hubei University
Wuhan 430062 (P. R. China)
E-mail: zmh@mailbox.gxnu.edu.cn
F. Yu,[+] Z.-H. Zhu, Dr. M.-H. Zeng
Department Key Laboratory for the Chemistry and Molecular Engineering of Medicinal Resources, School of Chemistry and Pharmaceutical Sciences Guangxi Normal University
Guilin 541004 (P. R. China)
Dr. Z.-W. Ouyang, Dr. Z. Wang
Wuhan National High Magnetic Field Center & School of Physics
Huazhong University of Science and Technology
Wuhan 430074 (P. R. China)
[+] These authors contributed equally to this work.
Supporting information and the ORCID identification number(s) for the author(s) of this article can be found under: https://doi.org/10.1002/anie.201813829.

ion. It has a central carbon atom (C55) attached to three 4-methyl-1-(1-methyl-1*H*-benzo[*d*]imidazol-2-yl)-4*H*-benzo-[d]imidazo[1,5-*a*]imidazolyl groups. These three heterocycles are held in a propeller-like conformation, which can be attributed to steric hindrance. The bond lengths of C55–C1 (1.427(5) Å), C55–C19 (1.417(5) Å), and C55–C37 (1.430-(5) Å) are between the values of C–C single (1.54 Å) and C=C double (1.34 Å) bonds. In addition, the maximum deviation from the least-squares plane through the central carbon atom (C55) and the three attached carbon atoms (C1, C19, and C37) is 0.051 Å for C55, indicating its planarity. These results suggest that the central carbon atom is sp^2-hybridized (Figure S1a and Table S1). Initially, compound **1** was assigned as $[C(C_{18}H_{14}N_5)_3]^+Cl^-\cdot 3\,CH_3OH$), and C55 is a carbocation balancing the negative charge of the Cl^- counterion. However, magnetism and electron paramagnetic resonance (EPR) experiments suggested that compound **1** has one unpaired electron (Figures 1 and S1). Thus **1** could be assigned as the $(C(C_{18}H_{14}N_5)HCl\cdot 3\,CH_3OH)$ ("hexamer" of **L1**), with a proton balancing the negative charge of Cl^-. It is worth noting that the dihedral angle between rings D and G (30.0°, Figure S1) is much larger than the other two corresponding dihedral angles (rings B and E: 10.3°; rings C and F: 15.4°). The considerable difference between these dihedral angles suggests the different steric hindrance between the heterocycles, which could be caused by the proton attached to N14 (Figure S1). Theoretical calculations on $C(C_{18}H_{14}N_5)_3H^+$ (simplified model of **1** by omitting the chloride counterion and solvent) at the DFT-B3LYP/6-31G(d) level of theory agree well with the crystal structure of **1**, and the corresponding dihedral angles are 20.2°, 6.1°, and 13.6°, respectively, suggesting that one of the N atoms is protonated (Table S2b).

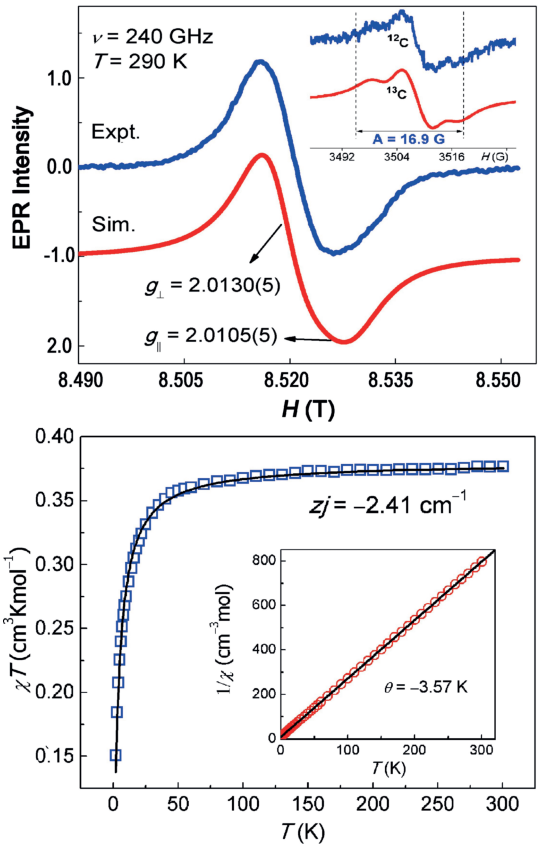

Figure 1. Top: EPR spectrum of compound **1**. Inset: EPR spectrum of ^{13}C-labeled **1** in the solid state (red: experimental, blue: simulation). Bottom: Temperature dependence of $\chi_m T$ for compound **1** at 0.1 T. Inset: $1/\chi_m$ vs. *T*. Solid lines represent the theoretical fits generated using the models discussed in the text.

The results of our magnetism and EPR experiments clearly suggested that **1** has one unpaired electron. The EPR spectrum features an asymmetric derivative peak, implying the existence of magnetic anisotropy in the molecule. Computational spectral simulations showed that the molecule has an axial magnetic anisotropy with $S = 1/2$, $g_\perp = 2.0130(5)$, and $g_\parallel = 2.0105(5)$. Hyperfine coupling of $^{13}C(\alpha)$ was found at room temperature with a hyperfine coupling constant of 16.9 G (Figure 1), which is close to the value obtained by theoretical calculations (10.7 G). The spin value is in good agreement with the values commonly measured for organic radicals,[10,11] confirming that **1** is a radical. The *g* value (2.012) is higher than those of other triarylmethyl free radicals (2.002–2.003), which could be partially ascribed to its nitrogen-rich character. Furthermore, the axial magnetic anisotropy of **1** agrees well with its planar structure. To study the electronic nature of **1**, the temperature dependence of the magnetic susceptibility was measured at 0.1 T as shown in Figure 1. The $\chi_m T$ value of 0.377 $cm^3\,K\,mol^{-1}$ at 300 K is close to the spin-only value of 0.375 $cm^3\,K\,mol^{-1}$ expected for one magnetically isolated magnetic center with $S = 1/2$ and $g = 2$, implying the existence of one unpaired electron in **1**. As the temperature is lowered, $\chi_m T$ gradually decreases to 0.15 $cm^3\,K\,mol^{-1}$ at 2 K, indicating the presence of antiferromagnetic coupling among the molecules. This is supported by the negative Weiss temperature $\theta = -3.57(5)$ K, obtained by fitting the $1/\chi_m$ versus *T* curve with the Curie–Weiss law between 30 and 300 K. The susceptibility of **1** was fitted using the PHI program with a model assuming that the decrease in $\chi_m T$ is due to intermolecular interactions. The resulting intermolecular interaction constant zJ amounts to −2.41-(2) cm^{-1}, which falls in the range of reported values for organic radicals.[10] The results of the theoretical calculations also suggest that compound **1** is a radical (Tables S2 and S3). The first stable triarylmethyl radical, the triphenylmethyl radical, was reported by Gomberg in 1900.[12] However, thus far, there are few examples of this type of radicals,[13,14] such as the tris(2,4,6-trichlorophenyl)methyl (TTM) radical, the perchlorotriphenylmethyl (PTM) radical, pyridyl-containing triarylmethyl radicals (PyBTM), the (*N*-carbazolyl)-bis(2,4,6-trichlorophenyl)methyl radical (CzBTM),[7] and the tri(9-anthryl)methyl radical.[15] Recently, 3-substituted 9-(naphthalen-2-yl)-9*H*-carbazole (3NCz) and 3-substituted 9-phenyl-9*H*-carbazole (3PCz) were introduced into the skeleton of TTM radical to give TTM-3-NCz and TTM-3PCz, respectively.[16] Compound **1** represents a new type of triarylmethyl radical containing different heterocycles. Furthermore, a solid sample of **1** could be stored in air at room temperature for months without appreciable decomposition, showing excellent stability.

Along with the generation of **1**, light yellow plate-like crystals were also formed in the reaction mixture. This

compound was characterized by NMR spectroscopy and high-resolution mass spectrometry and could be assigned to compound **2** ($C_{37}H_{30}N_{10}$; bis(4-methyl-1-(1-methyl-1*H*-benzo-[d]imidazol-2-yl)-4*H*-benzo[*d*]imidazo[1,5-*a*]imidazol-3-yl)methane). Crystals suitable for single-crystal X-ray diffraction were obtained by recrystallization of the crude crystals in a mixture of dilute hydrochloric acid and methanol. The C–C bond lengths around the central carbon atom are 1.506 Å, close to those of typical C–C single bonds, suggesting that the central carbon atom is sp^3-hybridized (Figure S1). Compound **2** consists of two 4-methyl-1-(1-methyl-1*H*-benzo-[*d*]imidazol-2-yl)-4*H*-benzo[*d*]imidazo[1,5-*a*]imidazolyl groups linked by the central carbon atom, and can be seen as a "tetramer" of the starting ligand **L1**. There are two Cl^- counterions in the crystal structure, and two N atoms (N1 and N1′) are protonated. The torsion angle of N1-C8-C9-N5 (−29.6°) is close to that in compound **1** (26.4°). Both compounds **1** and **2** consist of the same (4-methyl-1-(1-methyl-1*H*-benzo[*d*]imidazol-2-yl)-4*H*-benzo[*d*]imidazo-[1,5-*a*]imidazolyl) groups, a "dimer" of **L1**, indicating that this "dimer" could be the synthon to produce compounds **1** and **2**. Fortunately, this "dimer", compound **3** ($C_{18}H_{15}N_5$), was successfully synthesized from **L1** by using isopropanol (*i*-PrOH) as the solvent (Figure S2 and Table S4). In the solid state, the dihedral angle between the two heterocycles in **3** is 12.9°, which is in the range of those in **1** (10.3–30.0°). The two coordinating N atoms are located on either side of the C–C bond connecting the two heterocycles, which can be ascribed to the steric hindrance between the methyl substituent and the H atom of the phenyl group. In addition, when the reaction of **L1** with $FeCl_3{\cdot}6H_2O$ in MeOH was carried out at room temperature, the complex $[Fe^{III}(\mathbf{L1})_2Cl(OCH_3)]Cl$ (**4**; Figure S3) was obtained. Its structure clearly shows that two **L1** ligands coordinate to the Fe^{III} cation. It is worth noting that compounds **1** (the "hexamer"), **2** (the "tetramer"), and **3** (the "dimer") were formed from relatively simple substrate **L1** under solvothermal conditions. A series of transformations should be involved in this reaction, which needed further study.

To gain more insight, ESI-MS was applied to track the reaction process. First, at room temperature, the fragment $[Fe^{II}(\mathbf{L1})_2Cl]^+$ and other fragments containing [Fe(**L1**)] moieties were detected, indicating the coordination of Fe^{3+} with **L1** (Figure S4 and Table S5). Then, under microwave-assisted solvothermal conditions, as shown in Figure 2 (and Figure S5 and Table S6), the representative fragments corresponding to **1** (*m*/*z* 912.3748, $[\mathbf{1}]^+$), **2** (*m*/*z* 613.2596, $[\mathbf{2}]^+$), **3** (*m*/*z* 302.1315, $[\mathbf{3}{+}H]^+$), and **4** (*m*/*z* 413.0942, $[Fe^{II}(\mathbf{L1})_2Cl]^+$) were detected. Initially, the abundances of $[\mathbf{3}{+}H]^+$ and $[Fe^{II}(\mathbf{L1})_2Cl]^+$ increased, but after 8 min, they began to decrease. The abundance of **1** increased gradually during the reaction course and that of **2** was low, which could be ascribed to its low solubility. Furthermore, two key fragments corresponding to $[(\mathbf{3}{-}H)CH_2OH + H]^+$ (*m*/*z* 332.1508) and $[(\mathbf{3}{-}H)_2CHOH{+}H]^+$ (*m*/*z* 631.2692) were also detected (Figure S6).

Control experiments were also performed to gain more information (Table S7 and Figure S7). First, without $FeCl_3{\cdot}6H_2O$, no fragments corresponding to compounds **1**, **2**, or **3** were detected, indicating that the metal salt is a prerequisite (Figure S7 a), which may activate the ligand by coordination. Interestingly, when **3** was heated in MeOH without $FeCl_3{\cdot}6H_2O$ (Figure S7 b) under solvothermal conditions (140 °C), the fragments of **1** and **2** were detected, indicating that once **3** has been formed, $FeCl_3{\cdot}6H_2O$ is not indispensable for the subsequent transformations. Furthermore, **1** and **2** were also detected under two other reaction conditions, namely upon 1) treating **L1** with HCHO in *i*-PrOH in the presence of $FeCl_3{\cdot}6H_2O$ (Figure S7 c); and upon 2) treating **3** with HCHO in *i*-PrOH without $FeCl_3{\cdot}6H_2O$ (Figure S7 d). These results also suggest that the solvent MeOH may be transformed into HCHO and then participate in the reaction. It is worth noting that **2** could also be transformed into **1** without $FeCl_3{\cdot}6H_2O$ (Figure S7 e), indicating that **1** might originate from **2**. When the reaction was carried out in the presence of DMPO (2,2,6,6-tetramethylpiperidine 1-oxyl), the peaks of **1** were not detected (Figure S7 f). This clearly confirmed that the reaction involves a radical pathway.

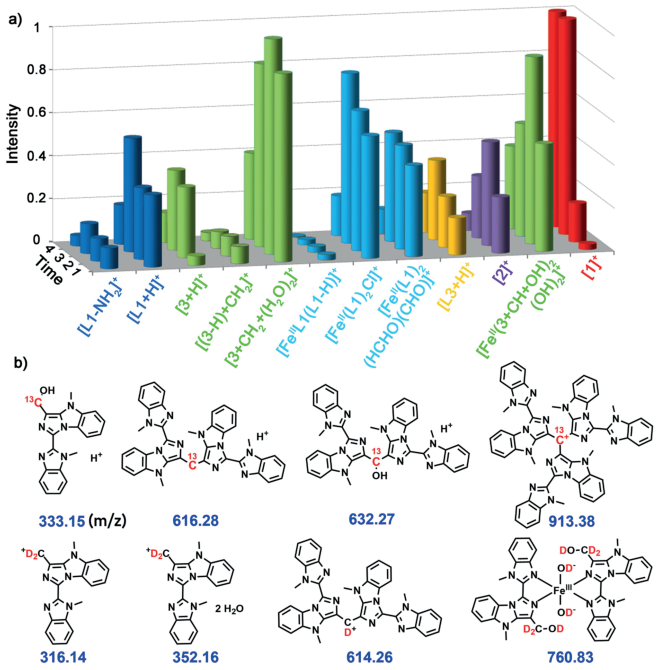

Figure 2. a) Relative intensities of the three systems during the assembly process at different points in time (1: 2 min; 2: 4 min; 3: 8 min; 4: 15 min) under ambient conditions. b) MS fragment assignment of key intermediates in isotope labeling experiments ($^{13}CH_3OH$ and CD_3OD).

To further confirm the source of the central carbon atom, isotope labeling experiments using $^{13}CH_3OH$ and CD_3OD as the solvent were carried out. The ^{13}C-labeled species $\mathbf{1}^*$, $\mathbf{2}^*$, $(\mathbf{3}{-}H)^{13}CH_2OH$, and $(\mathbf{3}{-}H)_2{}^{13}CHOH$ were detected ($[\mathbf{1}^*]^+$: 913.3781 (*m*/*z*), $[\mathbf{2}^*{+}H]^+$: 616.2771, $[(\mathbf{3}{-}H)^{13}CH_2OH{+}H]^+$: 333.15, $[(\mathbf{3}{-}H)_2{}^{13}CHOH{+}H]^+$: 632.27; Figure 2 b and Figure S8). The deuterated fragments (*m*/*z* 316.14, *m*/*z* 352.16, *m*/*z* 614.26, and *m*/*z* 760.83) were also detected (Figures 2 b and S8 and Table S8). All of these results confirmed the hypothesis that methanol is the source of the central carbon atom. As an abundant chemical feedstock, methanol can be used as a C_1 building block in C–C and C–N bond formation;

however, coupling reactions between aromatic carbon atoms and methanol are very rare.[17] Radical **1** represents the first example of a free radical derived from the sequential cleavage of the four bonds around the carbon atom of methanol.

From the synthesis of **3** and the control experiments, a plausible mechanism is proposed (Figure 3a). Ligand **L1** coordinates with $FeCl_3{\cdot}6H_2O$ to give intermediate $[Fe^{II}(\mathbf{L1})_2Cl]^+$ (step i). The self-condensation of the coordinated

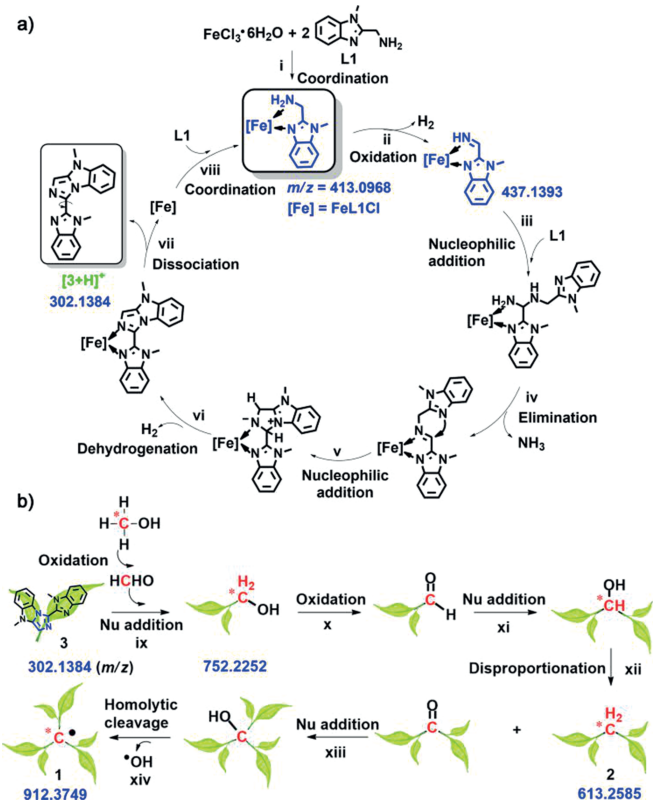

Figure 3. Plausible mechanisms for the formation of **3** (a) and **1** (b).

L1 to an imine (ii–iv) is followed by intramolecular cyclization (v), aromatization (vi), and dissociation (vii) to give **3**.[18] Then, **3** could react with formaldehyde (viii) derived from methanol to give a primary alcohol (ix; Figure 3b). This primary alcohol could be oxidized to an aldehyde (x), which could undergo nucleophilic addition with **3** to produce a secondary alcohol (xi). This secondary alcohol could disproportionate to **2** and a ketone (xii). Then, the ketone could again undergo nucleophilic addition with **3** to give a tertiary alcohol (xiii), which could undergo homolytic cleavage of the C–O bond to afford the free radical **1** (xiv). Finally, free radical **1** could combine with a HCl molecule present in the reaction system to give the final product, free radical cation [**1**]·HCl. This reaction meets the criteria of domino reactions. Although the classification of the reaction steps in this domino reaction is not straightforward, based on the chemical bond breaking and forming, this is a 14 step domino reaction.[19] This sequence involves more steps than the longest previously reported 12 step cascade reaction.[6a] While the previously reported radicals were synthesized by oxidation of the corresponding carbanions with I_2 or *p*-chloranil (Table S9), our new radical was prepared by C–O homolytic cleavage, which represents a new pathway to give a carbon-centered free radical.

In summary, we have described the synthesis of a novel organic free radical **1** with high stability under microwave-assisted solvothermal conditions at 140 °C. The new method is different from the common procedure for generating such radicals, which involves the oxidation of the corresponding carbanion at room temperature or even lower temperature. Ligand **L1** underwent a series of transformations, including coordination, self-condensation, cyclization, aromatization, and triple coupling with the solvent methanol followed by C–O homolytic cleavage to produce **1** via the key intermediates **4**, "dimer" **3**, and "tetramer" **2**. Even with such a large series of reaction steps, the yield of free radical **1** was still as high as 30%, and the atom economy of the domino reaction is as high as 91.8%. This domino reaction, thus far the longest reported (14 steps), was thoroughly studied through the combination of crystallography and ESI-MS techniques. This combination of techniques shows great usefulness in tracking complicated reaction processes even for the rare circumstance in which the solvent takes part in the reaction. To the best of our knowledge, this is the first time that a triarylmethyl free radical has been produced by the homolytic cleavage of a C–O bond, which is different from the traditional oxidation of a carbanion and provides a new strategy to synthesize free radicals. The participation of the solvent methanol, which undergoes multiple activations of the four bonds around the C atom, is attractive and inspiring for the synthesis of organic macromolecules.

Acknowledgements

This work was supported by the National Science Foundation of China for Distinguished Young Scholars (Grant 21525101), the NSF of Hubei Province innovation group project (2017CFA006), the BAGUI scholar program (2014A001), NSFGX (Grants 2014GXNSFFA118003, 2017GXNSFDA198040). The National High Magnetic Field Laboratory is supported by the National Science Foundation through NSF/DMR-1157490/1644779 and the State of Florida.

Conflict of interest

The authors declare no conflict of interest.

Keywords: domino reactions · mass spectrometry · radicals · solvothermal methods · X-ray diffraction

How to cite: *Angew. Chem. Int. Ed.* **2019**, *58*, 3748–3753
Angew. Chem. **2019**, *131*, 3788–3793

[1] D. Schröder, *Acc. Chem. Res.* **2012**, *45*, 1521–1532.
[2] a) H. N. Miras, L. Cronin, *New Strategies in Chemical Synthesis and Catalysis*, Wiley-VCH, Weinheim, **2012**; b) S. Datta, M. L.

Saha, P. J. Stang, *Acc. Chem. Res.* **2018**, *51*, 2047 – 2063; c) D. J. Tranchemontagne, J. L. Mendoza-Cortés, M. O'Keeffe, O. M. Yaghi, *Chem. Soc. Rev.* **2009**, *38*, 1257 – 1283.
[3] a) P. J. Kitson, G. Marie, J.-P. Francoia, S. S. Zalesskiy, R. C. Sigerson, J. S. Mathieson, L. Cronin, *Science* **2018**, *359*, 314 – 319; b) T. G. Saint-Denis, R.-Y. Zhu, G. Chen, Q.-F. Wu, J.-Q. Yu, *Science* **2018**, *359*, eaao4798; c) Q. F. Sun, S. Sato, M. Fujita, *Nat. Chem.* **2012**, *4*, 330 – 333.
[4] a) L. F. Tietze, *Chem. Rev.* **1996**, *96*, 115 – 136; b) L. F. Tietze, B. Waldecker, D. Ganapathy, C. Eichhorst, T. Lenzer, K. Oum, S. O. Reichmann, D. Stalke, *Angew. Chem. Int. Ed.* **2015**, *54*, 10317 – 10321; *Angew. Chem.* **2015**, *127*, 10457 – 10461; c) P. Chauhan, S. Mahajan, D. Enders, *Acc. Chem. Res.* **2017**, *50*, 2809 – 2821.
[5] a) H. Dückert, V. Pries, V. Khedkar, S. Menninger, H. Bruss, A. W. Bird, Z. Maliga, A. Brockmeyer, P. Janning, A. Hyman, *Nat. Chem. Biol.* **2011**, *8*, 179 – 184; b) Y. Ishida, I. Nakamura, M. Terada, *J. Am. Chem. Soc.* **2018**, *140*, 8629 – 8633.
[6] J.-P. Zhong, B. Liu, T. Yang, Y.-J. Liu, M.-H. Zeng, B.-F. Shi, M. Kurmoo, *Inorg. Chem.* **2017**, *56*, 10123 – 10126.
[7] X.-M. Chen, M.-L. Tong, *Acc. Chem. Res.* **2007**, *40*, 162 – 170.
[8] M.-H. Zeng, Z. Yin, Z.-H. Liu, H.-B. Xu, Y.-C. Feng, Y.-Q. Hu, L.-X. Chang, Y.-X. Zhang, J. Huang, M. Kurmoo, *Angew. Chem. Int. Ed.* **2016**, *55*, 11407 – 11411; *Angew. Chem.* **2016**, *128*, 11579 – 11583.
[9] a) Y.-Q. Hu, M.-H. Zeng, K. Zhang, S. Hu, F.-F. Zhou, M. Kurmoo, *J. Am. Chem. Soc.* **2013**, *135*, 7901 – 7908; b) H.-X. Na, P.-Y. Yang, Z. Yin, Y.-H. Wang, L.-X. Chang, R. Si, M. Kurmoo, M.-H. Zeng, *Chem. Eur. J.* **2016**, *22*, 18404 – 18411; c) H.-L. Zheng, X.-L. Chen, T. Li, Z. Yin, Y. Zhang, M. Kurmoo, M.-H. Zeng, *Chem. Eur. J.* **2018**, *24*, 7906 – 7912.
[10] T. T. Tidwell in *Encyclopedia of Radicals in Chemistry, Biology and Materials*, *Vol. 1*, Wiley, Hoboken, **2012**, pp. 1 – 35.
[11] a) X. Ai, Y. Chen, Y. Feng, F. Li, *Angew. Chem. Int. Ed.* **2018**, *57*, 2869 – 2873; *Angew. Chem.* **2018**, *130*, 2919 – 2923; b) W. Wang, C. Chen, C. Shu, S. Rajca, X. Wang, A. Rajca, *J. Am. Chem. Soc.* **2018**, *140*, 7820 – 7826.
[12] M. Gomberg, *J. Am. Chem. Soc.* **1900**, *22*, 757 – 771.
[13] a) Y. Hattori, T. Kusamoto, H. Nishihara, *Angew. Chem. Int. Ed.* **2014**, *53*, 11845 – 11848; *Angew. Chem.* **2014**, *126*, 12039 – 12042; b) D. Velasco, S. Castellanos, M. López, F. López-Calahorra, E. Brillas, L. Juliá, *J. Org. Chem.* **2007**, *72*, 7523 – 7532; c) S. Dong, A. Obolda, Q. Peng, Y. Zhang, S. Marder, F. Li, *Mater. Chem. Front.* **2017**, *1*, 2132 – 2135.
[14] a) A. Heckmann, S. Dümmler, J. Pauli, M. Margraf, J. Köhler, D. Stich, C. Lambert, I. Fischer, U. Resch-Genger, *J. Phys. Chem. C* **2009**, *113*, 20958 – 20966; b) M. A. Fox, E. Gaillard, C. C. Chen, *J. Am. Chem. Soc.* **1987**, *109*, 7088 – 7094.
[15] T. NIshiuchi, S. Aibara, T. Kubo, *Angew. Chem. Int. Ed.* **2018**, *57*, 16516 – 16519; *Angew. Chem.* **2018**, *130*, 16754 – 16757.
[16] X. Ai, E. W. Evans, S. Dong, A. J. Gillett, H. Guo, Y. Chen, T. J. H. Hele, R. H. Friend, F. Li, *Nature* **2018**, *563*, 536 – 540.
[17] Y. Chen, L. Li, Y. Cao, J. Wu, Q. Cao, Y. Li, H. Hu, W. Liu, Y. Liu, Z. Kang, J. Li, *CrystEngComm* **2013**, *15*, 2675 – 2681.
[18] Y. Chen, L. Li, Z. Chen, Y. Liu, H. Hu, W. Chen, W. Liu, Y. Li, T. Lei, Y. Cao, Z. Kang, M. Lin, W. Li, *Inorg. Chem.* **2012**, *51*, 9705 – 9713.
[19] N. J. Green, C. A. Connolly, K. P. W. Rietdijk, G. S. Nichol, F. Duarte, A. L. Lawrence, *Angew. Chem. Int. Ed.* **2018**, *57*, 6198 – 6202; *Angew. Chem.* **2018**, *130*, 6306 – 6310.

Manuscript received: December 5, 2018
Accepted manuscript online: December 27, 2018
Version of record online: January 21, 2019

